Microsyst Technol (2010) 16:657–668
DOI 10.1007/s00542-009-1000-5

TECHNICAL PAPER

Vibration energy scavenging via piezoelectric bimorphs of optimized shapes

Denis Benasciutti · Luciano Moro · Saša Zelenika · Eugenio Brusa

Received: 14 July 2009 / Accepted: 15 December 2009 / Published online: 30 December 2009

Abstract Compact autonomous power sources are one of the prerequisites for the development of wireless sensor networks. In this work vibration energy harvesting via piezoelectric resonant bimorph beams is studied. The available analytical approaches for the modeling of the coupled electromechanical behavior are critically evaluated and compared with a finite element (FEM) numerical model. The latter is applied to analyze thoroughly the stress and strain states, as well as to evaluate the resulting voltage and charge distributions in the piezoelectric layers. The aim of increasing the specific power generated per unit of scavenger volume is pursued by optimizing the shape of the scavengers. Two optimized trapezoidal configurations are hence identified and analyzed. An experimental set-up for the validation of the proposed numerical model and of the obtained optimized structures is developed. Results of a preliminary experimental assessment, confirming the improved performances of optimized scavengers, are finally given.

D. Benasciutti · L. Moro · S. Zelenika
Department of Electrical, Management and Mechanical Engineering (DIEGM), Tech-UP Laboratory, University of Udine, Via delle Scienze 208, 33100 Udine, Italy

S. Zelenika (✉)
Laboratory for Precision Engineering, Department of Mechanical Engineering Design, Faculty of Engineering, University of Rijeka, Vukovarska 58, 51000 Rijeka, Croatia
e-mail: sasa.zelenika@riteh.hr

E. Brusa
Laboratory of Microsystems Design and Characterization, Department of Mechanics, Politecnico di Torino, Corso Duca degli Abruzzi 24, 10129 Torino, Italy

1 Introduction

Pervasive technologies are one of the most challenging innovations in mechatronic systems aimed at distributed monitoring of the environment, of structures and of people. Ubiquous distributed low-power wireless sensors are already being often used to monitor mechanical and physical properties as well as damage in structures, industries or automobiles. They are also used in some critical environments as well as to monitor continuously the parameters relevant to the prevention of catastrophic events, the interruption of vital services or the advent of traumatic states and health risks for people (Helal et al. 2008; Priya and Inman 2009; Starner and Paradiso 2004).

One of the key features in the design of sensor networks is the possibility to supply the needed power over a large space. Currently available batteries do not comply with the requirements of autonomy and system miniaturization or wearability. A valid solution to this shortcoming was found in energy conversion of the power available in the same environment where the sensors are located. Harvesting of environmental energy that can have the form of photovoltaic, wind, electromagnetic radiation, thermoelectric, kinetic or other energy sources is hence increasingly studied (Starner and Paradiso 2004; Anton and Sodano 2007; Paradiso and Starner 2005).

The collocation of power sources and the respective sensors not only decreases energy losses in power transmission, but also assures a real-time supply and allows reducing the dimensions of the used devices. This can, in turn, enable the creation of wearable systems that, in the case of elder care technology, is used to transmit measurement data about some vital biometric parameters (acceleration, temperature or blood pressure) to medical personnel. The sensor, the processor and the communications unit all rely on

localized power generators, which must assure sufficient autonomy within the given volume and weight constrains. Miniaturized energy conversion systems are proposed to satisfy these requirements (Helal et al. 2008; Priya and Inman 2009).

Harvesting of kinetic energy (such as, for example, that of human motion, breathing or respiration) has recently gained particular attention. Especially relevant in this frame is the harvesting of vibration energy. In this instance power is generated in situ, often by converting kinetic energy of vibrating resonant structures into energy storage of electric charge (Priya and Inman 2009; Beeby et al. 2006; Renno et al. 2009). Among the proposed approaches, piezoelectric conversion is useful because of its inherent electromechanical coupling. What is more, in the case of micro-electro-mechanical systems (MEMS), it allows microfabrication and it assures good performances. These can be achieved, for instance, by cantilevers made of a metallic substrate with piezoelectric material surface bonded onto it. The structures usually vibrate at their first resonance frequency (Carson 1978; Genta 1998), while vibration is imposed by external environment or by people. Important contributions relating to the design of optimized piezoelectric vibration scavenging devices were identified in literature (Priya and Inman 2009; Erturk and Inman 2008, 2009; Goldschmidtboeing and Woias 2008; Guyomar et al. 2005; Mateu and Moll 2005; Roundy and Wright 2004; Roundy et al. 2005; Shahruz 2006) although a complete list of relevant design parameters and specifications is not available (i.e. some important optimization parameters, such as resonant frequency, volume, or maximum dimensions, are either not clearly stated or are not kept constant among the proposed geometries).

The design of piezoelectric vibration energy harvesting devices is therefore dealt with in this work with the aim of formulating suitable optimization criteria for obtaining the highest output power per unit of scavenger volume. Extending the approaches proposed in literature, the analysis of the studied devices is performed by means of a coupled electromechanical model taking into account all the main design parameters. Two trapezoidal optimized geometries are hence identified and compared to the conventional rectangular scavenger. The computational procedures proposed in the available analytical approaches (Guyomar et al. 2005; Roundy and Wright 2004; Erturk and Inman 2009) are hence implemented and validated via the newly developed numerical approach, based on the finite element method (FEM), that allows the coupling of the piezoelectric bimorph and of the downstream electrical load to be explicitly performed. In fact, the detailed design of the structure implies the need of a thorough analysis of the stress, strain and charge distributions on the piezoelectric transducer that can be poorly predicted by the analytical methods, since these are mainly focused on the evaluation of the average power output of the transducer. Moreover, an experimental apparatus for the validation of the proposed numerical approach and optimized scavenger shapes is set-up. It is thus proven that the proposed optimized layouts provide considerable improvements of energy harvesting performances.

2 Electromechanical behavior of bimorph vibration energy scavengers

A reference layout of the considered energy scavengers is shown in Fig. 1. The cantilever is excited at the fixed end at a given frequency and loaded at the free end with a proof mass, which can be suitably selected to adapt the resonant frequency of the system to that of excitation, thus maximizing transmissibility. Piezoelectric layers, indicated in Fig. 1 with 1, are surface bonded to the metallic shim indicated with 2. The strain of the piezoelectric material produced by vibrations is converted, via electromechanical coupling, into an electric charge distribution thus inducing an electric field between the upper and the lower electrode. In the following treatise, it is supposed that the two electrodes are connected to an external resistive load R_L. The condition of having a pure resistive load, although not necessarily the most realistic one (electric load often consists of rechargeable batteries or other capacitive loads), is very useful for an immediate comparison of the harvested power levels (Roundy and Wright 2004).

In the considered configuration, flexural excitation is preferred since several authors demonstrate that the corresponding "mode 31" of piezoelectric coupling assures the best energy conversion efficiency (Priya and Inman 2009; Roundy and Wright 2004). Since in real operation

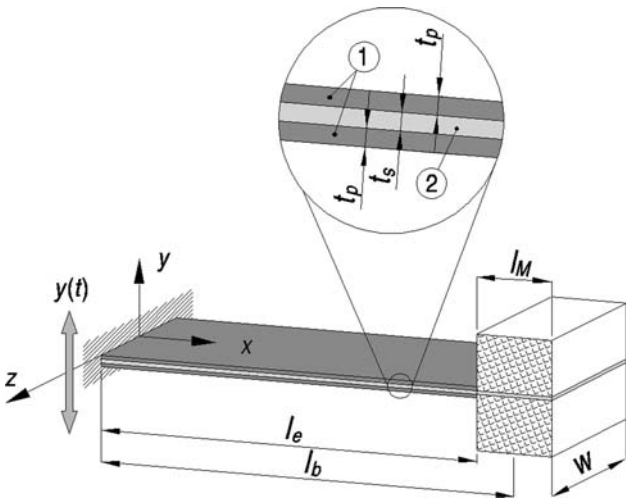

Fig. 1 Basic layout of the bimorph vibration energy scavenger

external excitation is predictable only with some degree of approximation, an eventual necessity to cover a determined frequency bandwidth can then be addressed either by employing an assembly of energy scavengers with close resonance frequencies (Shahruz 2006) or by applying a passive (Roundy et al. 2005) or an active (Brusa et al. 1998) tuning system.

The electromechanical behavior of the reference rectangular scavenger structure widely analyzed in literature and shown in Fig. 1 can be modeled by analytical approaches of different degrees of approximation.

2.1 Electromechanical model

In the analytical model developed by Guyomar and coworkers (Guyomar et al. 2005), the bimorph scavenger with proof mass M at its free end is represented as an equivalent mass-piezo-spring-damper system such as depicted in Fig. 2. With K is indicated here the stiffness of the scavenger and with c its viscous damping coefficient. External excitation, given by the force $F(t)$, results in a displacement $Y_{\mathrm{TIP}}(t)$ of mass M and is opposed by the restoring force $F_p(t)$ of the piezoelectric element, that of the equivalent spring, as well as the viscous force of the damper. $F(t)$ is supposed to be equal to the excitation acceleration A_{in} acting on the proof mass M, i.e. $F(t) = A_{\mathrm{in}}M$. The respective constitutive equations can hence be written as:

$$F_p(t) = K_p Y_{\mathrm{TIP}}(t) + \alpha V(t), \quad i(t) = \alpha \dot{Y}_{\mathrm{TIP}}(t) - C_p \dot{V}(t) \tag{1}$$

where K_p is the stiffness of the piezoelectric element, α is the so-called force factor and C_p is the piezoelectric capacitance. $i(t)$ and $V(t)$ indicate, respectively, the outgoing current and voltage on the piezoelectric element. The average power dissipated across the resistor R_L at the excitation frequency ω will then be given by:

$$P = \frac{|V|^2}{2R_L} = \frac{F^2}{2}\frac{R_L\alpha^2}{1+\left(\omega C_p R_{\mathrm{L}}\right)^2}\frac{1}{\left(c+\frac{R_L\alpha^2}{1+\left(\omega C_p R_L\right)^2}\right)^2} \tag{2}$$

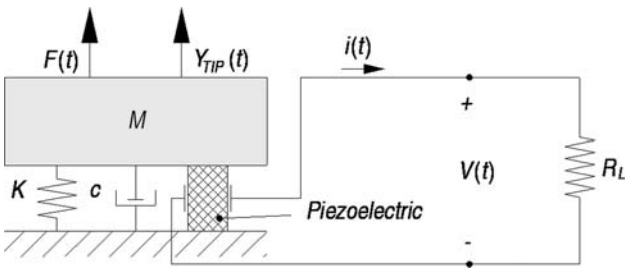

Fig. 2 Electromechanical model of the piezoelectric vibration energy scavenger

The average output power can thus be determined knowing the electrical parameters of the system and measuring its response, i.e. obtaining experimentally the values of F, c and α (Guyomar et al. 2005).

2.2 Single-degree-of-freedom equivalent circuit model

An analytical model which describes the behavior of the scavenger at its first flexural resonance frequency was developed by Roundy and Wright (Roundy and Wright 2004). The equivalent model shown in Fig. 3, obtained by employing electromechanical analogy (Crandall et al. 1968), is used to describe the behavior of the bimorph and to estimate the electric power generation. Each of the mechanical properties of the mechanical subsystem is hence replaced by an equivalent electric component. As an example, the bending stress $\sigma(x)$ induced by vibrations in a cross section at a distance x from the fixed end, is averaged on the electrode length and represented as a voltage generator $G(t)$. Similarly, L, C and R designate, respectively, the equivalent mechanical inertia, compliance and damping of the bimorph. The resulting dynamics can thus be represented as:

$$\begin{aligned} G(t) &= L\ddot{S}(t) + R\dot{S}(t) + \frac{S(t)}{C} + nV(t), \\ i(t) &= C_p\dot{V}(t) + \frac{V(t)}{R_L} \end{aligned} \tag{3}$$

where S represents mechanical strain, n is the equivalent turns ratio of the transformer used to represent electromechanical coupling while the other used symbols have the same meaning as in the case of the previous model.

In the flexural configuration (piezoelectric "mode 31"), the dependence of the electric voltage V across the piezoelectric layers on the mechanical bending stress σ is obtained via the piezoelectric coefficient d_{31} and is related also to Young's modulus and the thickness of the piezoelectric layer (Y_p and t_p respectively):

$$\sigma = -d_{31}\frac{aY_p}{2t_p}V \tag{4}$$

where a is equal either to 1 or 2 for piezoelectric layers connected, respectively in series or in parallel (Roundy and

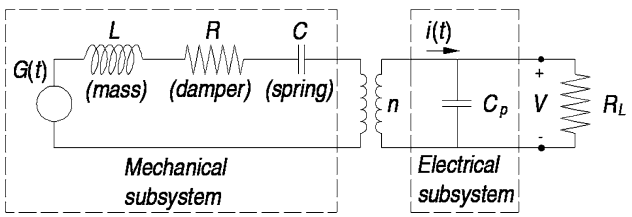

Fig. 3 Equivalent circuit model of the bimorph vibration energy scavenger

Wright 2004). Assuming a pure sinusoidal excitation displacement $y(t)$ at a frequency ω, the produced voltage V will thus be (Roundy and Wright 2004):

$$V = \frac{A_{\text{in}}}{k_2} \frac{j\omega \frac{2Y_P d_{31} t_p}{a\varepsilon^S}}{j\omega\left(k_{31}^2\omega^2 + \frac{2\zeta\omega}{R_L C_p}\right) - 2\zeta\omega^3} \tag{5}$$

where A_{in} is the amplitude of the excitation acceleration, ζ is the mechanical damping ratio, ε^S is the static permittivity of the piezoelectric material at constant strain, k_2 denotes a parameter related to the geometry of the cantilever, k_{31} is the electromechanical coupling coefficient while j is the imaginary unit. For a lumped parameter model, it is assumed here that the first flexural resonant frequency ω_n of the bimorph, tuned to external excitation, can be estimated as:

$$\omega_n = \sqrt{\frac{Y_p}{mk_1k_2}} \tag{6}$$

where k_1, similarly to k_2, is a parameter related to cantilever's geometry.

For each load R_L, the variation of the frequency ω will allow a maximum voltage V to be determined. The respective average power dissipated on the resistor will hence be:

$$P = \frac{|V|^2}{2R_L} \tag{7}$$

Although this model is simple, it allows the key parameters of electromechanical coupling to be appreciated. The coupling coefficient k_{31} is the relevant figure of merit for the efficiency of electromechanical coupling, while capacitance C_p is the key electric parameter for circuitry design.

2.3 Distributed parameters model

Although the above lumped parameter models provide useful insights into the dynamic behavior of electromechanical bimorphs and allow identifying the key features of power generation, they are characterized by some intrinsic drawbacks, as emphasized by Erturk and Inman (Erturk and Inman 2008). For example, lumped parameter models assume that the proof mass is dominant with respect to the mass of the bimorph cantilever. In practical applications this hypothesis is usually satisfied but, when the proof mass-to-cantilever mass ratio is not too large, appropriate corrections must be applied (Erturk and Inman 2008).

An alternative strategy recently proposed in literature is to adopt distributed parameter models. The approach proposed by Erturk and Inman (Erturk and Inman 2009) is hence based on the study of the deflections induced by the bending dynamics (i.e. mode shapes) of the cantilever and not on the generally adopted static considerations based on the Euler–Bernoulli beam equation. Furthermore, this distributed parameters model includes also a feedback from the electrical to the mechanical subsystem through piezoelectric coupling, which affects the mechanical dynamics of the scavengers (i.e. the resonant frequency depends on the applied resistive load).

In this case the behavior of the bimorph is hence described by a partial differential equation of motion, including appropriate dissipative terms (with coefficients c_a and c_s) (Erturk and Inman 2009):

$$\begin{aligned} &Y_p I \frac{\partial^4 w_{\text{rel}}(x,t)}{\partial x^4} + c_s I \frac{\partial^5 w_{\text{rel}}(x,t)}{\partial x^4 \partial t} + c_a \frac{\partial w_{\text{rel}}(x,t)}{\partial t} + m\frac{\partial^2 w_{\text{rel}}(x,t)}{\partial t^2} \\ &+ \vartheta V(t)\left[\frac{d\delta(x)}{dx} - \frac{d\delta(x-l_b)}{dx}\right] = -[m + M\,\delta(x-l_b)]\frac{\partial^2 y(t)}{\partial t^2} \end{aligned} \tag{8}$$

where $\delta(x)$ is the Dirac delta function, m is the beam mass per unit of length, M is the proof mass, $y(t)$ is the excitation displacement and ϑ is the backward coupling term. By expanding the expression for beam's deflection relative to its base as:

$$w_{\text{rel}}(x,t) = \sum_{r=1}^{\infty} \varphi_r(x)\eta_r(t) \tag{9}$$

in which $\eta_r(t)$ is the modal coordinate and $\phi_r(x)$ is the mode shape, the dynamic of the bimorph for the rth mode can be described by the set of coupled equations:

$$\begin{cases} \ddot{\eta}_r(t) + 2\zeta_r\omega_r\dot{\eta}_r(t) + \omega_r^2\eta_r(t) + \chi_r V(t) = f_r(t) \\ \dfrac{C_p}{2}\dot{V}(t) + \dfrac{V(t)}{R_L} = i(t) \end{cases} \tag{10}$$

where χ_r is a modal electromechanical coupling term correlated to the mode shape $\phi_r(x)$, ω_r is the resonant frequency and $f_r(t)$ is the modal mechanical forcing function. The other terms have the same meaning as those used in the above lumped parameter models. The first of Eq. 10 is the mechanical equation of motion in modal coordinates, while the second one is the electrical equation.

Under a pure sinusoidal excitation of the fixed end of the cantilever with a frequency ω close to the rth natural frequency ω_r, the electric voltage across the piezoelectric layers connected in series becomes:

$$V = \frac{j2\omega R_L \kappa_r F_r}{(2 + j\omega R_L C_p)(\omega_r^2 - \omega^2 + j2\zeta_r\omega_r\omega) + j2\omega R_L \kappa_r \chi_r} \tag{11}$$

where F_r is the amplitude of the modal mechanical forcing function and κ_r is a modal coupling term related to the mode shape $\phi_r(x)$.

3 Optimization of shape of bimorph vibration energy scavengers

Electromechanical coupling depends on electric capacitance which is, in turn, dependent on the area and the shape of the transducer itself. To maximize energy conversion, in literature it is thus suggested to cover the largest possible area of the device with piezoelectric material (Crawley and Hall 1991). However, if the surface of the cantilever is covered by the piezoelectric material regardless of the strain state, overall performance can be limited, since the highest conversion can be achieved only if the piezoelectric material is strained in every portion of the layer close to its strength limits. Moreover, given that the charge resulting from mechanical strain anywhere on the layer will be uniformly distributed on it, an averaging effect is obtained.

The design goal is therefore that of shaping the surface of the piezoelectric layer so that, for a vibration mode chosen for energy scavenging, the piezoelectric material is situated in correspondence of strain concentrations on beam's surface. Each mode would hence imply a different optimized scavenger shape. However, when the main aim is making use of the first bending resonance of the cantilever, as is the case considered in this work, the criterion of uniform strength seems appropriate, as it allows storing within the material the highest possible elastic potential energy (Carson 1978; Genta 1998). For a given load condition, the geometry of the structure is therefore herein designed to approximate as much as possible a constant stress state on the beam.

In the conventional rectangular scavenger the bending moment and the resulting normal stress decrease linearly from the fixed to the free end. On the other hand, a triangular beam shape allows obtaining a uniform stress distribution along the cantilever surface. Given the necessary place for the fixation of the proof mass and other technological constraints, this optimized shape is approximated by a trapezoidal one referred to in the following as "trapezoidal shape". An interesting and innovative alternative could be represented by clamping the narrow end of the trapezoid, i.e. using a "reversed trapezoidal shape"; this increases significantly the stress at the fixation, while the larger area at the free end will be weakly stressed but it facilitates the positioning of the proof mass. According to the outlined criteria, the trapezoidal and the reversed trapezoidal shapes are given in Fig. 4.

These two devices have a variable width $w(x)$ along the beam. For a given cross section location x, the corresponding width, as function of beam length l_b, for the trapezoidal and the reversed trapezoidal shape, will respectively be:

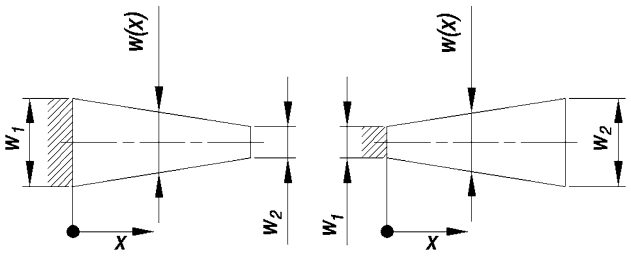

Fig. 4 "Trapezoidal" (*left*) and "reversed trapezoidal" (*right*) scavenger shapes clamped along the side of width w_1 and with the proof mass (not shown for clarity reasons) affixed at the free end of width w_2

$$w(x) = \frac{(w_1 - w_2)(l_b - x)}{l_b} + w_2, \qquad w(x) = \frac{(w_2 - w_1)x}{l_b} + w_1 \tag{12}$$

Stresses σ and their distributions along the scavenger length for a given proof mass were computed for the trapezoidal shape of decreasing w_2 and constant w_1, while these bounds were inversed in the case of the reversed trapezoidal shape. The obtained results are compared in Fig. 5 in terms of the dimensionless stress (with F being the inertial load due to the proof mass, while the cantilever dimensions are referred to Fig. 1) as function of x.

It can be noted that the reversed layout provides a fairly large stress at the fixation, although this is concentrated and decreases quickly along the beam length. The highest stress values may even be above the ultimate strength of the material and turn out to be critical for the fatigue lifetime of the device. The trapezoidal shape provides, in turn, a more uniform distribution with the maximum stress much lower than in the previous case.

3.1 Optimized shapes

A rectangular shaped energy scavenger replicating the typical geometry of Fig. 1 is taken as reference for this study. It is constituted by a metallic structure made of stainless steel, while the considered piezoelectric material is PSI-5A4E lead–zirconate–titanate (PZT) commercialized by Piezo Systems Inc. (Piezo Systems, http://www.piezo.com). The piezoelectric layers are supposed poled for series operation, since this configuration provides the highest voltage between the electrodes of the two layers bonded on the beam structure. The respective characteristics used in this work are given in Table 1.

According to the above remarks, geometric requirements on scavenger shapes include the values of piezoelectric layers' surface area and maximum width. To investigate the role of these two parameters, optimized geometries having either the same maximal width or the

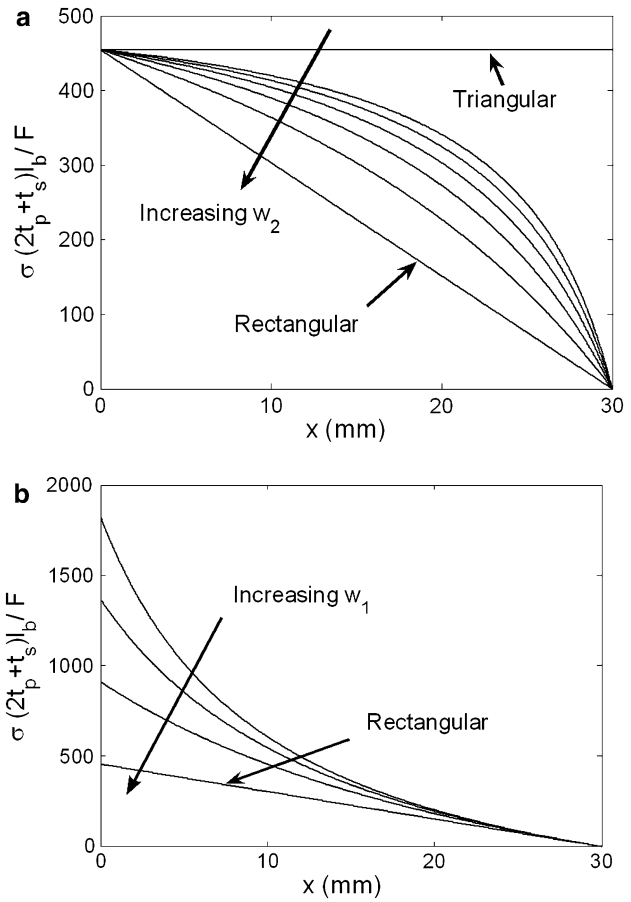

Fig. 5 Stress distributions along the scavenger length computed for the "trapezoidal" (**a**) and the "reversed trapezoidal" (**b**) scavenger shape for a constant inertial force

Table 1 Main geometry and material characteristics of the reference structure

Parameter	Value
Length of proof mass	$l_M = 10$ mm
Length of electrode for rectangular shape	$l_e = 25$ mm
Width of beam for rectangular shape	$w = 14$ mm
Thickness of metallic layer	$t_s = 0.1$ mm
Thickness of piezoelectric layer	$t_p = 0.2$ mm
Density of piezoelectric material	$\rho_p = 7.8$ g/cm^3
Young's modulus of piezoelectric material	$Y_p = 6.6 \times 10^4$ MPa
Young's modulus of steel	$Y_s = 2.06 \times 10^5$ MPa
Electromechanical coupling coefficient	$k_{31} = 0.3$
Permittivity of free space	$\varepsilon_0 = 8.8542 \times 10^{-12}$ F/m
Static permittivity at constant stress	$\varepsilon^T = 1{,}800\ \varepsilon_0$ F/m

same total volume of the piezoelectric material are compared. In a first instance, a maximal transversal dimension of a determined value w is thus assumed for the rectangular, trapezoidal and reverse trapezoidal shapes. In the second case the widths w_1 and w_2 of both trapezoidal configurations are varied while keeping constant the volume of all considered scavenger shapes. Since the capacitance of the piezoelectric transducer depends on its surface, the two approaches give different results.

In Fig. 6 are shown the top view drawings with the main dimensions of the optimized prototypes; the remaining geometric and material characteristics are identical to those of the rectangular shape and are listed in Table 1. The optimized cantilevers are designed so as to keep constant the first flexural eigenfrequency, described for the reference rectangular scavenger by Eq. 6. A typical value of 50 Hz, corresponding to the vibrations induced by sources in the domestic and industrial environments, is selected, while the inertial load is constituted by a cubic 10 gram mass. All bimorph cantilevers are then excited at their resonance frequency with a sinusoidal acceleration of amplitude 2 m/s^2.

As shown above, the performance of the scavengers will depend on the applied resistive load. In Fig. 7 are thus shown the scavenged specific powers per unit of piezoelectric material volume as function of the connected resistances obtained by employing the SDOF equivalent circuit model described in Sect. 2.2. The diagrams correspond to the layouts given in Fig. 6. The efficiency of prototypes c and d seems clearly better. All the curves in Fig. 7 are obtained by using a different value of eigenfrequency for each applied resistive load R_L, i.e. the backward electromechanical coupling is duly taken into account, although this meaningful aspect is generally neglected in available literature.

It is worth noting here that the values of the harvested power obtained in the present study are approximately

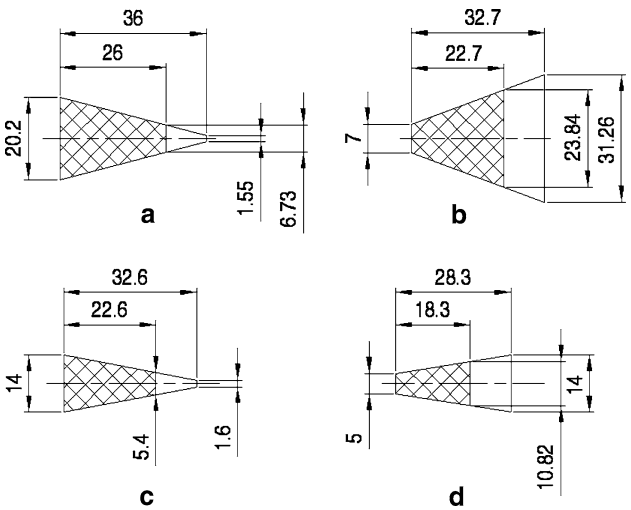

Fig. 6 Optimized scavenger prototypes having equal resonance frequency and equal volumes (**a**, **b**) or equal maximum transversal widths (**c**, **d**)

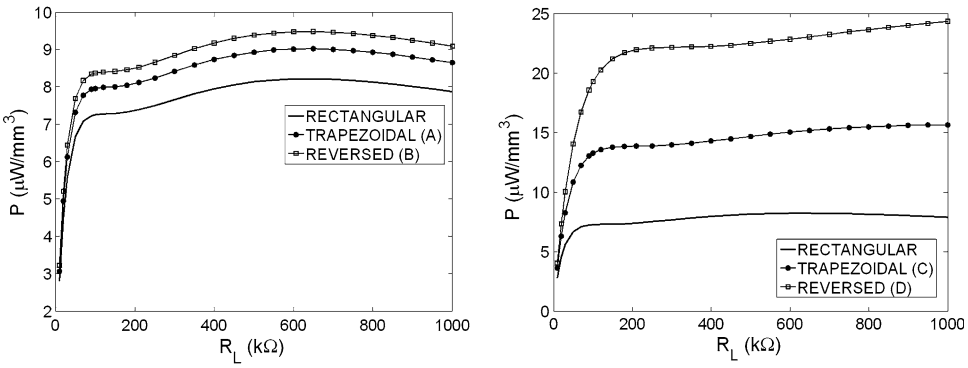

Fig. 7 Specific powers obtained on the scavengers of optimized shapes

comparable to the data reported in literature (Roundy and Wright 2004; Beeby et al. 2006); however, a precise comparison is difficult, due to the difference in geometry and excitation accelerations.

3.2 FEM modeling of optimized layouts

The above described analytical models available in literature (Guyomar et al. 2005; Roundy and Wright 2004; Erturk and Inman 2009), although helpful in defining relevant parameters for the harvested power levels, are somewhat simplified from the structural point of view. In order to obtain a more detailed description of the electromechanical behavior of the system, involving effects such as stress concentration and charge distribution, accurate analyses, as for example by means of FEM, should be performed.

A coupled-field electromechanical FE model is hence developed by means of the commercial ANSYS code. A 3D model is built with SOLID45 elements for the metallic structure and the inertial mass and SOLID5 elements for the two piezoelectric layers, for a total of 22,780 electric and mechanical degrees of freedom (DOFs). As shown in Fig. 8, the piezoelectric layers are connected via the electric circuit elements CIRCU94, representing a resistor.

In a first step, a modal analysis of all optimized scavenger shape configurations is performed to calculate their natural frequencies and eigenmodes. As an example, in Fig. 9 are shown the first four modes of vibration of the scavenger with reversed trapezoidal shape (respectively at 50, 210, 312 and 2,370 Hz—values close to these are obtained for the other shapes as well). It is worth noting here that the sequence of computed eigenmodes in the frequency domain includes a second torsional mode. However, resonance frequencies are well separated and external actions can thus be clearly applied to the first eigenmode without exciting torsional vibrations.

To calculate the power generated on the studied geometries, a forced dynamic (harmonic) analysis is implemented

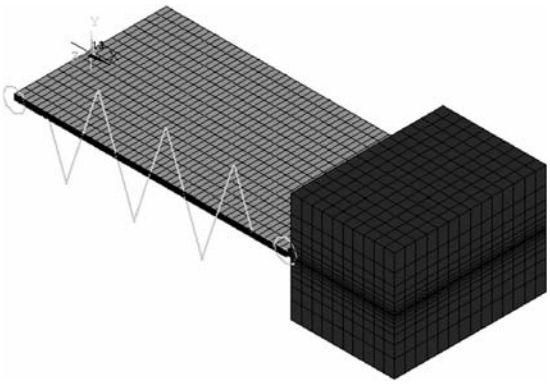

Fig. 8 Coupled-field FE model of the rectangular scavenger

next. Excitation of sinusoidal form is applied at the cantilever fixed end assuming constant excitation acceleration amplitude while maintaining the excitation frequency equal to the resonance frequency. The displacements along the cantilever are computed allowing, by employing coupled electromechanical analysis, the stress and the charge distributions on the piezoelectric layers to be identified. This, in turn, allows the voltage and scavenged power estimation.

Using the chosen FEM code it is possible to perform also the computation of the variation of the voltage and power distributions by varying the applied resistive loads (see Fig. 8). The resulting power values versus the resistive load on the rectangular scavenger are shown in Fig. 10a, where the marked similarity, but also the differences, due to the evidenced limits of the models illustrated in Sect. 2, can be appreciated. The approximations of the described SDOF equivalent circuit model give rise to an overestimate of the calculated specific power levels per unit of the piezoelectric material volume. The electromechanical model, on the other hand, gives results slightly lower than the numerical ones. In this case the amplitude of the displacements Y_{TIP} are those calculated via FEM harmonic analysis. The distributed parameters model allows results which are very close to FEM results, both in terms of

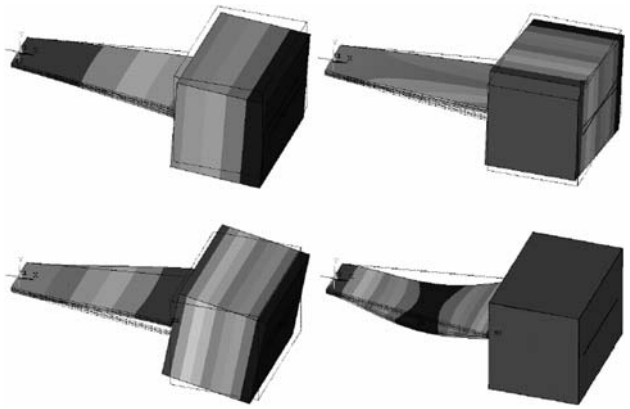

Fig. 9 First four vibration modes of the reversed trapezoidal (D) scavenger

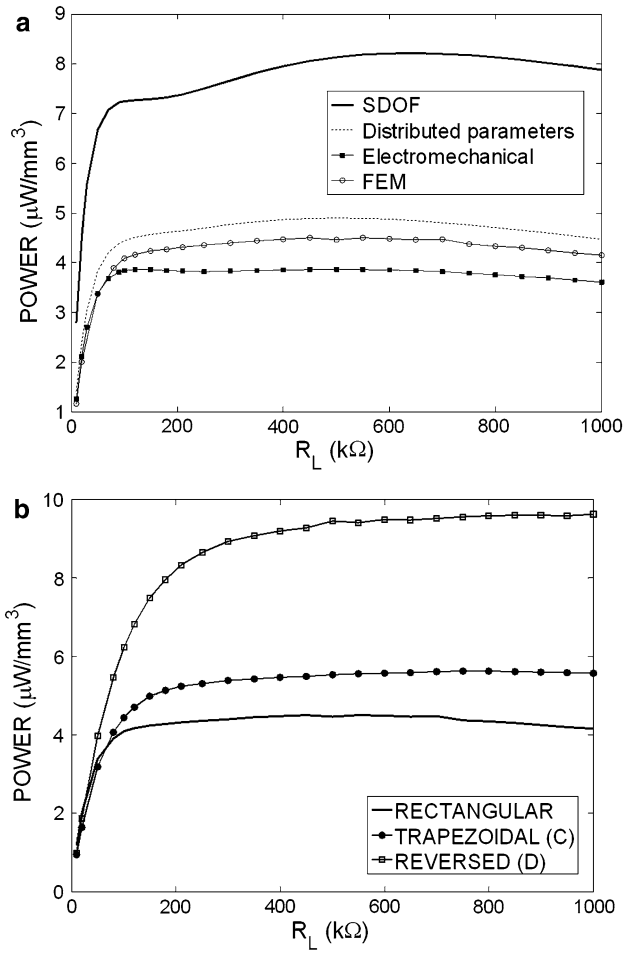

Fig. 10 FEM and analytical variations of the specific power on the rectangular scavenger for variable resistive loads (**a**) and FEM results for the scavenger shapes of equal maximum transversal widths (**b**)

values and overall trends, to be obtained. The results for the scavenger shapes of equal maximal widths calculated by employing FEM are shown in Fig. 10b and have the same trends of those given in Fig. 7.

3.3 Obtained results

In Fig. 11 are shown the voltage distributions along the considered scavenger shapes resulting from FEM analyses. It can be observed that these follow the stress distributions given in Fig. 5. A smoother voltage distribution on the surface of the piezoelectric layers is obtained in the case of trapezoidal shapes. However, the efficiency of trapezoidal shapes is affected by the clamp. In fact, the width of this shape is large at the fixed end where the fixation causes a lowering of the voltage levels which is reflected also in the average values for the whole bimorph. This effect, which cannot be appreciated by using the models described in Sect. 2, affects also the mode shape of the trapezoidal scavengers. All of this causes a lowering of the obtainable power levels that can be appreciated also by comparing Fig. 10b and Fig. 7. and could indicate that it might be better not to clamp the piezoelectric layers but only the metallic shim. In the case of the reversed trapezoidal configurations, a charge peak, corresponding to the highest stresses at the fixation of the cantilever, is obtained. In this region the width of the scavenger is small but, since the contribution of this peak to the average voltage on the bimorph is significant, clamping has a significant effect on the average achievable powers for the reversed trapezoids as well.

Although the capacitance of the transducer depends on its surface, and thus the shapes having equal volume ought to give similar electric capacitances, due to the marked difference in charge distribution, this is not the case. This reflection is qualitative in nature, since the surface electrode covers the whole piezoelectric layer and its high conductivity distributes immediately the charge. Nevertheless, it is evident that the voltage distributions shown in Fig. 11 differ sufficiently to give the designers additional parameters to refine the performed optimization.

In Table 2 are shown the relevant values for the comparison of the performances of the proposed geometries with respect to the reference rectangular configuration. The maximal scavenged specific powers per unit of volume are almost 10 $\mu W/mm^3$.

FEM analyses confirm thus a significant increase of energy scavenging in case of the optimized geometric configurations of equal maximal widths with respect to the conventional rectangular shape. In this case the limitations due to the clamping effect are thus largely compensated by a better usage of the material, i.e. higher average strain levels. The highest improvement (up to more than 100%!) in specific power per unit of piezoelectric material volume is obtained in the case of the reversed trapezoidal shape, although a very marked advantage is obtained also by using the trapezoidal shape of equal maximal width. The equal volume criterion, contrary to what the models described in

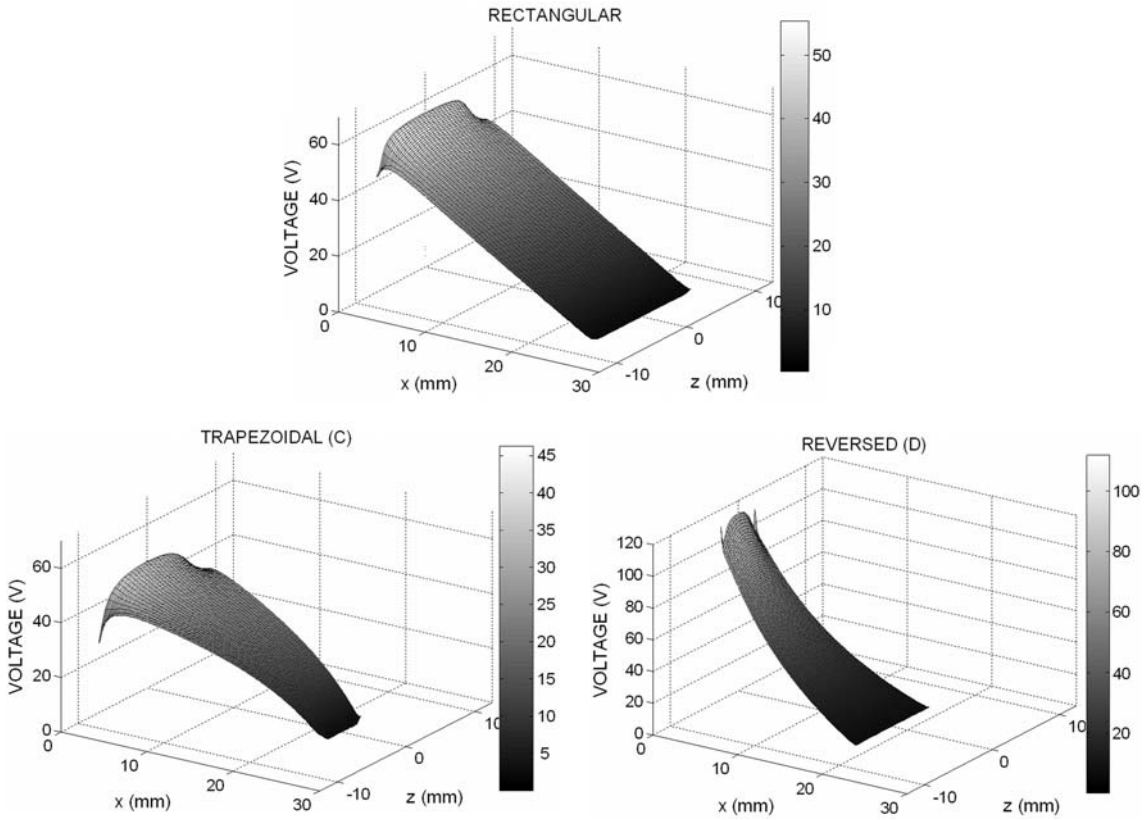

Fig. 11 Voltage distributions at the surface of the considered energy scavenger shapes

Table 2 Results of the FEM analyses on the proposed geometries

	Rectangular	Equal volume		Equal max. widths	
		Trap. (A)	Rev. trap. (B)	Trap. (C)	Rev. trap. (D)
Max. power FEM ($\mu W/mm^3$)	4.5	3.9 (−13.3%)	4.2 (−6.7%)	5.6 (+24%)	9.6 (+113%)
Average open circuit voltage FEM (V)	54	50 (−7%)	46.2 (−4.4%)	60.3 (+11.7%)	72.6 (+34%)

Sect. 2 would predict, results in a lowering of the obtained specific powers mostly due to the effects of the cantilever fixation visible in Fig. 11.

All of this brings a noteworthy new insight in the criteria to be adopted in the design of optimized piezoelectric vibration energy harvesting devices, and thus extends significantly the notions so far only marginally elaborated in the relevant literature.

4 Experimental set-up and preliminary measurements

An experimental apparatus for a preliminary validation of the numerical model developed in this study is set-up (Fig. 12). Specimens are made of two PSI-5A4E 0.2 mm thick PZT layers surface bounded on a 0.1 mm thick stainless steel shim and poled for series operation (Piezo Systems). The samples loaded with a suitable proof mass are excited via a PM25 MB Dynamics shaker. Excitation can be set at a given frequency imposing concurrently a constant acceleration or a constant displacement. For these purposes the shaker is driven by a 2635 Brüel & Kjaer amplifier and a 1047 Brüel & Kjaer exciter controller. Excitation acceleration is measured by 4375 Brüel & Kjaer accelerometers, while the resistive loads are adjusted via potentiometers. Displacements of the scavenger tip are monitored via a Micro-Epsilon OptoNCDT 1605 laser measurement system. All the data, including the obtained voltages, are collected via a PXI-1042 National Instruments data acquisition system and elaborated by employing LabVIEW-based algorithms.

In a first instance the electric characteristics of the piezoelectric transducers are measured employing a Hewlett-Packard 4284 capacitance measurement system. By measuring the capacitance and resistance (i.e. impedance) for variable excitation frequencies, it is verified that the

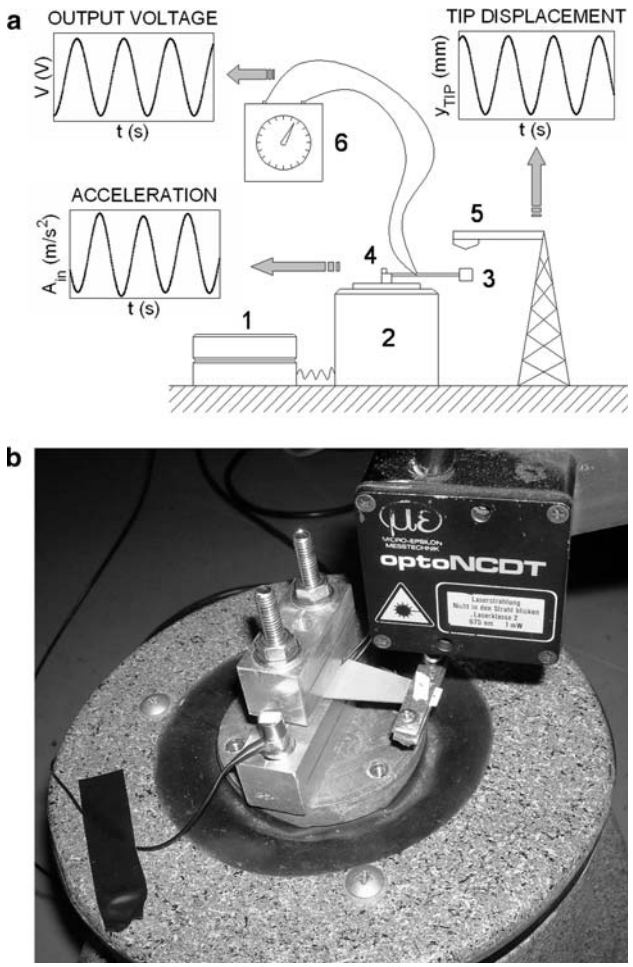

Fig. 12 Scheme of the experimental set-up (**a**): signal generator and amplifier (*1*), shaker (*2*), bimorph with proof mass (*3*), accelerometer (*4*), laser (*5*), resistive load (*6*); photo of the actual set-up (**b**)

transducer behave as a pure capacitor (i.e. that the resistive and inductive components of the transducer behavior are negligible), while, as shown in Fig. 13, its impedance is inversely proportional to excitation frequency (Law et al. 1996).

It is to be noted, however, that in the definition of equivalent capacitance not only the material but also the conditions of usage have to be taken into account. In fact, the capacitance of a single piezoelectric layer of surface area A and thickness t_p will be:

$$C_b = \frac{\varepsilon^T A}{t_p} \tag{13}$$

where ε^T is the permittivity of the piezoelectric material free of bounds at constant stress. When the piezoelectric layers are mechanically constrained, as in the herein considered case, the equivalent capacity diminishes (Smits et al. 1991). In this case the permittivity to be considered must be that at constant strain, given as:

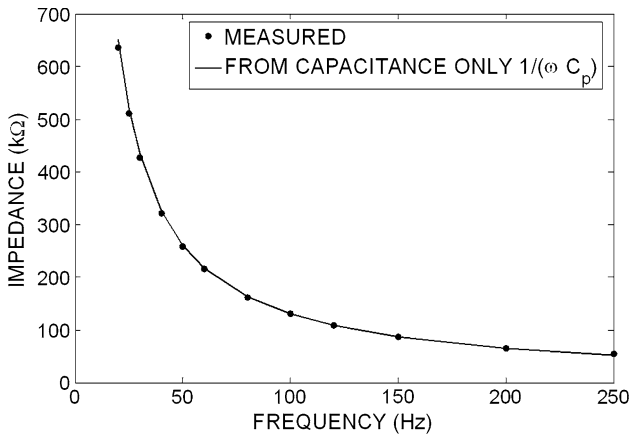

Fig. 13 Impedance of optimized energy scavengers

$$\varepsilon^S = \varepsilon^T\left(1 - k_{31}^2\right) \tag{14}$$

The importance of these parameters is evident considering the capacitance values given in Table 3.

By measuring the acceleration of the fixation of the bimorphs via the accelerometer and concurrently the displacement of its free end via the laser system, the typical transmissibility curves are obtained. These allow evaluating the mechanical damping ratio ζ of the studied structures, which is thus determined to be about 1.5%.

Fixing then preliminarily the excitation acceleration at a cautious amplitude level of 0.65 m/s^2, while the resistive load R_L is varied from 31 to 660 kΩ, a sine sweep is performed to determine each respective eigenfrequency. In fact, it is to be noted that Young's modulus of the piezoelectric material, and thus its dynamic response, vary, although moderately, for changing resistive loads (Law et al. 1996). The values of the output voltage corresponding to the eigenfrequency for a specific resistive load are thus measured.

Concerning the electromechanical coupling coefficient k_{31}, the conventional expression (Roundy and Wright 2004)

$$k_{31}^2 = \frac{\omega_{oc}^2 - \omega_{sc}^2}{\omega_{oc}^2} \tag{15}$$

cannot be used if only the metallic shim is clamped at the fixed end. In fact, the small difference between the open circuit resonance frequency ω_{oc} and the short circuit resonance frequency ω_{sc} would result in a coupling coefficient value $k_{31} = 0.14$. Only by clamping the piezoelectric layers of the bimorph, the difference between the mentioned frequencies is such that the measured value of coupling coefficient is $k_{31} = 0.3$, i.e. close to the nominal value of $k_{31} = 0.35$. The coupling is thus much better in the latter case.

Table 3 Comparison of capacitance values

	Capacitance (*nF*)		
	Calculated with ε^T	Calculated with ε^S	Measured
Rectangular	13.95	12.69	12.3
Trapezoidal (C)	9.06	8.24	7.9
Reversed trapezoidal (D)	11.14	10.13	9.8

Preliminary results in terms of the obtained specific average output powers from the considered scavenger configurations at the mentioned lower accelerations than those taken into consideration in Figs. 7 and 10 (0.65 vs. 2 m/s^2), are reported in Fig. 14. It can be clearly seen that the experimental curves have the same trends as the theoretical ones and that the trapezoidal shape produces significantly higher powers than the rectangular one. The somewhat different form of the curves in Fig. 14 with respect to those in Fig. 10b is due to the fact that during the preliminary measurements reported here, the piezoelectric layers have not been clamped.

A comparison between numerical simulations and experimental measurements for the reference rectangular cantilever is given in Fig. 15 in terms of the voltage frequency response function (FRF) versus the excitation frequency. As it can be seen, a close agreement is achieved in the whole frequency range of interest, while, due to the mentioned reversed piezoelectric coupling effect, the usual approach (Roundy and Wright 2004) of adopting a single frequency for the assessment of the power levels is clearly proven of limited use. A sine sweep for each value of the R_L load is hence to be preferred in practice.

The experimental set-up is still in development and thus the systematic validation of the studied specimens is ongoing. The problems to be still dealt with include a more elaborated control of the clamping at the fixed end of the cantilever. This includes also a validation of the necessity to clamp the piezoelectric layer itself, as supposed in the models described in Sect. 2 and substantiated also by some of the considerations resulting from the measurements, but that could induce fatigue lifetime limitations and enhance the problems outlined in Fig. 11. The fastening of the proof mass so as to guarantee reproducible resonance frequencies, to avoid eventual short circuits, as well as to inhibit eventual parasitic influences of secondary vibration modes, is also an issue. Nonetheless, the analytical, numerical and experimental results obtained so far clearly show that, in terms of generated power, optimized piezoelectric energy scavenger shapes could lead to significantly better specific performances.

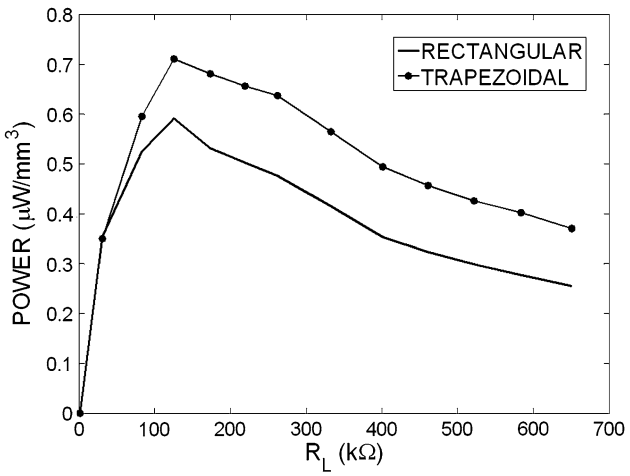

Fig. 14 Specific average output powers obtained on the studied scavenger shapes

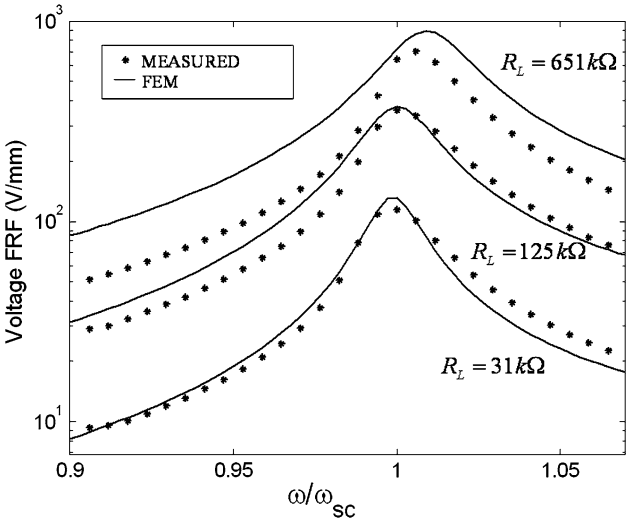

Fig. 15 Voltage frequency response function of the rectangular scavenger: comparison between FE numerical calculations and experimental measurements

5 Conclusions

The recent increased attention dedicated to wireless sensor networks for environmental and elder care monitoring requires a corresponding development of portable power generation and accumulation devices called energy scavengers. In this work the electromechanical optimization of the shapes of bimorph cantilever resonators able to convert environmental vibrations into electrical energy is performed. Two trapezoidal configurations, having respectively the wider side clamped or free, are proposed. Models given in literature are applied to obtain a preliminary evaluation of the scavenged powers. A numerical model, developed by using the FEM, and taking into account all the

relevant structural and electromechanical coupling effects, is then implemented. It is thus shown that the proposed geometries with equal maximal widths, if compared to the reference rectangular shape, allow considerable gains in the achieved power levels. The reached specific powers per unit of volume seem compatible with the power requirements of currently used wireless sensors. A preliminary experimental campaign on energy scavenger prototypes demonstrated the validity of the developed numerical model as well as the better performances of the optimized trapezoidal scavenger shapes, evidencing, however, several important electromechanical phenomena to be duly taken into account. A thorough experimental analysis is currently being carried on. The work will then proceed by considering the possibility of including passive and active tuning of the resonances of optimized devices to assure the maximal energy scavenging regardless of the uncertainties in the design and fabrication parameters, in the constraint conditions and in the excitation frequencies. The analyses will certainly have to include also material strength limits.

Acknowledgments This work is supported by the "TECH-UP" project for the development of pervasive technologies of the Friuli Venezia Giulia Region, Italy, the "Ultra-high precision compliant devices for micro and nanotechnology applications" project of the Croatian Ministry of Science, Education and Sports and the "Theoretical and Experimental Analysis of Compliant Mechanisms for Micro- and Nanomechanical Applications" project of the Italian Ministry of University and Research. The authors wish to acknowledge also the important contribution of Mr. Elvio Castellarin in the execution of the experimental measurements.

References

Anton SR, Sodano HA (2007) A review of power harvesting using piezoelectric materials (2003–2006). Smart Mater Struct 16:R1–R21

Beeby SP, Tudor MJ, White NM (2006) Energy harvesting vibration sources for microsystems applications. Meas Sci Technol 17:R175–R195

Brusa E, Carabelli S, Carraro F, Tonoli A (1998) Electromechanical tuning of self-sensing piezoelectric transducers. J Intell Mater Sys Struct 9:198–209

Carson J (1978) Springs design handbook. Dekker

Crandall SH et al (1968) Dynamics of mechanical and electromechanical systems. McGraw-Hill, New York

Crawley E, Hall S (1991) The dynamics of controlled structures, vol 1–3. Technical Course, MIT, Boston

Erturk A, Inman DJ (2008) Issues in mathematical modeling of piezoelectric energy harvesters. Smart Mater Struct 17(6):065016

Erturk A, Inman DJ (2009) An experimentally validated bimorph cantilever model for piezoelectric energy harvesting from base excitation. Smart Mater Struct 18(2):025009

Genta G (1998) Vibrations of structures and machines. Springer, New York

Goldschmidtboeing F, Woias P (2008) Characterization of different beam shapes for piezoelectric energy harvesting. J Micromech Microeng 18:104013

Guyomar D, Badel A, Lefeuvre E, Richard C (2005) Toward energy harvesting using active materials and conversion improvement by nonlinear processing. IEEE Trans Ultrason Ferroelecr Freq Control 52(4):584–595

Helal A, Mokhtari M, Abdulrazak B (2008) The engineering handbook of smart technology for aging, disability and independence. Wiley, New York

Law HH, Rossiter PL, Simon GP, Koss LL (1996) Characterization of mechanical vibration damping by piezoelectric materials. J Sound Vibr 197(4):378–402

Mateu L, Moll F (2005) Optimum piezoelectric bending beam structures for energy harvesting using shoe inserts. J Intell Mater Sys Struct 16:835–845

Paradiso JA, Starner T (2005) Energy scavenging for mobile and wireless electronics. IEEE Pervasive Comput 4(1):18–27

Priya S, Inman D (eds) (2009) Energy harvesting technologies. Springer, New York

Renno JM, Daqaq MF, Inman DJ (2009) On the optimal energy harvesting for a vibration source. J Sound Vibr 320:386–405

Roundy S, Wright PK (2004) A piezoelectric vibration based generator for wireless electronics. Smart Mater Struct 13:1131–1142

Roundy S et al (2005) Improving power output for vibration-based energy scavengers. IEEE Pervasive Comput 4(1):28–36

Shahruz SM (2006) Limits of performance of mechanical band-pass filters used in energy scavenging. J Sound Vibr 293:449–461

Smits JG, Dalke SI, Cooney TK (1991) The constituents equations of piezoelectric bimorphs. Sens Actuators A Phys 28:41–61

Starner T, Paradiso JA (2004) Human generated power for mobile electronics. In: Piguet G (ed) Low power electronics design, chap 45. CRC Press, Boca Raton